
Article:
Verbruggen, S.W. orcid.org/0000-0002-2321-1367, Vaughan, T.J. and McNamara, L.M. (2016) Mechanisms of osteocyte stimulation in osteoporosis. Journal of the Mechanical Behavior of Biomedical Materials, 62. pp. 158-168. ISSN 1751-6161

https://doi.org/10.1016/j.jmbbm.2016.05.004

Mechanisms of Osteocyte Stimulation in Osteoporosis

Stefaan W. Verbruggen, Ted J. Vaughan, Laoise M. McNamara

Biomechanics Research Centre (BMEC), Biomedical Engineering,

College of Engineering and Informatics,

National University of Ireland, Galway

Address for correspondence:

Dr. Laoise M. McNamara

Department of Biomedical Engineering

National University of Ireland Galway

Galway,

Ireland

Phone: (353) 91-492251

Fax: (353) 91-563991

Email: Laoise.McNamara@nuigalway.ie

Key words of the paper: Bone, osteocyte, mechanobiology, lacuna, osteoporosis

ABSTRACT

Experimental studies have shown that primary osteoporosis caused by oestrogen-deficiency results in localised alterations in bone tissue properties and mineral composition. Additionally, changes to the lacunar-canalicular architecture surrounding the mechanosensitive osteocyte have been observed in animal models of the disease. Recently, it has also been demonstrated that the mechanical stimulation sensed by osteocytes changes significantly during osteoporosis. Specifically, it was shown osteoporotic bone cells experience higher maximum strains than healthy bone cells after short durations of oestrogen deficiency. However, in long-term oestrogen deficiency there was no significant difference between bone cells in healthy and normal bone. The mechanisms by which these changes arise are unknown. In this study, we test the hypothesis that complex changes in tissue composition and lacunar-canalicular architecture during osteoporosis alter the mechanical stimulation of the osteocyte. The objective of this research is to employ computational methods to investigate the relationship between changes in bone tissue composition and microstructure and the mechanical stimulation of osteocytes during osteoporosis. By simulating physiological loading, it was observed that an initial decrease in tissue stiffness (of 0.425 GPa) and mineral content (of 0.66 wt% Ca) relative to controls could explain the mechanical stimulation observed at the early stages of oestrogen deficiency (5 weeks post-OVX) during in situ bone cell loading in an oestrogen-deficient rat model of post-menopausal osteoporosis (Verbruggen et al. 2015). Moreover, it was found that a later increase in stiffness (of 1.175 GPa) and mineral content (of 1.64 wt% Ca) during long-term osteoporosis (34 weeks post-OVX), could explain the mechanical stimuli previously observed at a later time point due to the progression of osteoporosis. Furthermore, changes in canalicular tortuosity arising during osteoporosis were shown to result in increased osteogenic strain stimulation, though to a lesser extent than has been observed experimentally. The findings of this study indicate that changes in the extracellular environment during

osteoporosis, arising from altered mineralisation and lacunar-canalicular architecture, lead to altered mechanical stimulation of osteocytes, and provide an enhanced understanding of changes in bone mechanobiology during osteoporosis.

1. INTRODUCTION

Bone is a highly adaptive tissue that can respond to changes in mechanical loading by altering the composition or structure of the bone. It is believed that bone cells can appraise their mechanical environment, through molecule or protein complexes known as mechanosensors, and produce certain biochemical signals (mechanotransduction) to initiate an adaptive response. Bone lining cells, osteoblasts and osteocytes, have been proposed to act as mechanosensors within bone tissue (Cowin et al. 1991; Lanyon 1993; Mullender and Huiskes 1997). Osteocytes are the most widely accepted candidates for sensing mechanical stresses in bone (Ajubi et al. 1996; Burger and Veldhuijzen 1993a; Carter and Caler 1985; Cowin et al. 1991; Huiskes et al. 2000; Klein-Nulend et al. 1995; Lanyon 1993; Mullender and Huiskes 1995; Mullender and Huiskes 1997; Mullender et al. 1994; Smit and Burger 2000; Weinbaum et al. 1994; Westbroek et al. 2000).

Osteoporosis is a disease that causes significant bone loss, micro-architectural deterioration and degradation of macroscopic bone properties (Compston et al. 1989; Parfitt 1987). It has also been shown that complex changes in the tissue level mechanical properties and composition occur following oestrogen deficiency in both the tibia and femur in animal models (Brennan et al. 2011b; McNamara et al. 2006). Specifically, it was seen that mechanical properties of trabecular bone in tibiae of ovariectomized rats are altered over time compared to sham-operated controls (McNamara et al. 2006; McNamara and Prendergast 2005). Similarly, the distribution of tissue-level mineral changes in the femur of a sheep model of osteoporosis (Brennan et al. 2011a), and changes in mineralized crystal maturity, mineral-to-matrix ratio, and collagen cross-linking also occur (Brennan et al. 2012). Interestingly tissue mineral

changes during oestrogen deficiency do not occur ubiquitously, but are more prevalent at specific anatomical regions within the femora of rat and ovine models of osteoporosis (Brennan et al. 2011a). Given that diminished levels of circulating oestrogen are systemic during osteoporosis, these local variations in bone composition and remodelling activity (i.e. the coordinated bone formation by osteoblasts and resorption by osteoclasts) were at first surprising. A recent study sought to establish the sequence with which complex changes in molecular and cellular biology, tissue composition, tissue integrity and architecture arise in the bone loss cascade of osteoporosis (McNamara 2010). It was proposed that the complex heterogeneous changes in bone tissue composition might be explained by the mechanical environment, which varies considerably in magnitude according to anatomical location.

A recent experimental study developed and applied novel confocal microscopy and digital image correlation techniques to characterise the mechanical environment of bone cells from an ovariectomized (OVX) rat model of osteoporosis in situ (Verbruggen et al. 2015). It was shown that bone cells from OVX bone tissue experienced higher maximum strains than sham-operated (SHAM) healthy bone cells after a short duration of oestrogen deficiency (5 weeks). Interestingly, this effect was mitigated in long-term oestrogen deficiency (34 weeks), whereby there was no longer a significant difference between bone cells in healthy and osteoporotic bone (Verbruggen et al. 2015). Thus we proposed that a mechanobiological response may occur, as a result of the increased cell stimulation experienced in early oestrogen deficiency, to return mechanical stimuli on osteocytes to control levels. Specifically, we proposed that this response may be manifested as an increase in bone tissue stiffness and mineral content, which has been observed previously in trabecular bone (Brennan et al. 2011a; McNamara et al. 2006). However, this theory remains unproven as the correlation between changes in bone tissue stiffness, mineral content and mechanical stimulation at the level of the osteocyte has not yet been established.

As well as the macroscopic and tissue level changes in bone tissue properties during osteoporosis, alterations in the local osteocyte environment have been observed. In particular it has been demonstrated that the lacunar-canalicular network in cortical bone in humans with osteoporosis is disorganised, with a more tortuous canalicular anatomy compared to healthy subjects (Knothe Tate et al. 2002; Knothe Tate et al. 2004). As demonstrated previously through the use of computational models to replicate the osteocyte mechanical environment (Anderson and Knothe Tate 2008; Kamioka et al. 2012; Verbruggen et al. 2012; Verbruggen et al. 2013), osteocyte stimulation is highly sensitive to the surrounding lacunar-canalicular architecture. Therefore, this increase in tortuosity during osteoporosis would likely affect the mechanical stimulation of the osteocyte in vivo, although this effect remains to be elucidated.

The objective of this study was to apply computational models to investigate potential mechanisms for experimental observations of altered in vivo osteocyte stimulation in bone cells from an ovariectomized (OVX) rat model of osteoporosis. This was done by (1) applying finite element (FE) models to determine the correlation between changes in bone tissue properties and osteocyte mechanical stimulation during osteoporosis, and (2) applying computational fluid-structure interaction (FSI) methods to explore the effect of alterations in the lacunar-canalicular anatomy on the local osteocyte mechanical environment.

2. MATERIALS AND METHODS

This study firstly used a finite element (FE) approach to investigate the effects of changes in bone tissue properties on osteocyte stimulation. Secondly, a fluid-structure interaction (FSI) approach was applied to investigate whether changes in the lacunar-canalicular architecture alter the mechanical stimulation of osteocytes during osteoporosis. These data were compared to data from a previously published study, which showed the micromechanical environment of

osteoblasts and osteocytes is altered in an animal model of short- and long-term osteoporosis (Verbruggen et al. 2015) and the relevant methods are described below.

2.1. Data from animal model and micromechanical loading/confocal microscopy

Experimental data from a previous study using an ovariectomised rat model of osteoporosis was employed in this analysis (Verbruggen et al. 2015). Briefly, the animals for this study consisted of four groups of 8-month old female Wistar rats; 1) a group in which rats were ovariectomised five weeks prior to the experiment (OVX-5, n=4) to induce oestrogen deficiency, 2) a control sham-operated group (SHAM-5, n=4), and a 34-week postoperative 3) ovariectomised (OVX-34, n=2) and 4) a corresponding control sham-operated group (SHAM-34, n=2). To visualize the local mechanical environment of the cells, a loading device compatible with a confocal microscope was designed, which was used to apply microscale displacements (at strain increments as small as 50 με) to fluorescently stained cortical bone samples from the femur and confocal imaging was simultaneously performed. Digital image correlation techniques were applied to characterise cellular strains. This study provided the first direct experimental data for the local mechanical environment of osteocytes and osteoblasts in situ during oestrogen deficiency (Verbruggen et al. 2015).

2.2. Finite element model to investigate the effects of altered bone tissue properties on osteocyte mechanical stimulation

2.2.1. FE model generation

Finite element models, described in detail in a previous study (Verbruggen et al. 2012), were employed to investigate the effects of alterations in material properties on the strain stimulation experienced by the osteocyte. Briefly, these models were derived from confocal laser scanning microscopy images of fluorescein isothiocyanate (FITC)-stained osteocyte lacunae, and thereby closely represent their geometry in vivo (see Figure 1). The confocal scans were taken

from the mid-diaphysis of the femur, and are thus from a similar location to those imaged during the experimental study described in (Verbruggen et al. 2015). Confocal image stacks of four osteocyte lacunae were imported into MIMICS image processing software (Materialise, Leuven, Belgium) and thresholded to between -884 and -769 Hounsfield units to generate three-dimensional solid models. These geometries were then meshed using 4-noded C3D4 tetrahedral elements and implemented using ABAQUS (Dassault Systemes, Vélizy-Villacoublay, France) finite element software.

The calcified extracellular matrix (ECM) model was constructed using a Boolean subtraction of the confocal image-derived geometries. Additionally, the osteocyte geometry was offset by 0.08 μm to create a pericellular space and a proteoglycan pericellular matrix (PCM) of the same thickness was constructed by Boolean subtraction. All materials were assumed to be isotropic and linear elastic. The elastic moduli of the solid continuum ECM and osteocyte models were assumed to be 16 GPa and 4.5 kPa respectively, with Poisson's ratios of 0.38 and 0.3 (Deligianni and Apostolopoulos 2008; Sugawara et al. 2008). As there is no experimental data on the material properties of the PCM surrounding the osteocyte at present the properties of chondrocyte PCM, were assumed with an elastic modulus of 40 kPa and Poisson's ratio of 0.4 (Alexopoulos et al. 2003; Alexopoulos et al. 2005). While the PCM of chondrocytes differs from that of osteocytes in that it contains collagen, proteoglycans are the primary feature of both (Sauren et al. 1992; Wilusz et al. 2014; You et al. 2004). Therefore we have assumed these values for the osteocyte PCM.

2.2.2. Parameter variation study of elastic moduli

Previous in vitro cell culture studies have established 10,000 με in bone cells as a threshold above which an osteogenic response is stimulated (Burger and Veldhuijzen 1993b; You et al. 2000). In order to determine whether changes in strain observed in our previous experimental

study (Verbruggen et al. 2015) could explore the possible mechanical properties in the computational model that could predict the observed experimental results. Specifically, the elastic modulus was altered incrementally from the initial value of 16 GPa until the proportion of the cell experiencing strains in the osteogenic range (under the applied loading conditions described below) matched that of the experimental results for the healthy (SHAM-5 and SHAM-34 weeks) and osteoporotic (OVX-5 and OVX-34 weeks) bone across four representative models. A Poisson's ratio of 0.38 was assigned to the ECM for each of these models.

2.2.3. Boundary conditions and loading

Initially, a pressure condition was applied to an ECM surface, which was gradually ramped up until strain stimulation equivalent to a 3,000 με compressive displacement load was achieved. The magnitude of the pressure load was then maintained at this level in order to simulate the loading applied in the experimental study (Verbruggen et al. 2015). While in vivo loading is of bone is dynamic and cyclic (Fritton et al. 2000), we have assumed linear elastic behaviour for the osteocyte due to its long relaxation time (41.5 s) relative to average frequency of physiological loading (~1 s) (Appelman et al. 2011; Darling et al. 2008), thus allowing simplification of loading to uniaxial ramped static loading. Loading was applied symmetrically, while simultaneously constraining the opposing faces symmetrically to prevent rigid body motion. Tie constraints were applied to attach the PCM to the ECM and osteocyte where direct contact occurred at their respective surfaces.

2.2.4. Correlation of elastic moduli to experimental measures of tissue mineralisation

To elucidate whether the changes in elastic moduli investigated in Section 2.2.2 above could be related to experimentally reported changes in tissue mineralisation (Brennan et al. 2009;

Brennan et al. 2011b; Busse et al. 2009), the resulting elastic moduli were then converted to a corresponding calcium content using a previously developed power law equation (Currey 1988):

$$\log(E) = -9.16 + 4.30\log(Ca)$$

where E denotes the elastic modulus and Ca denotes calcium content. These values for calcium content were then converted to weight percentage calcium (wt% Ca).

2.3. Fluid-structure interaction modelling to investigate the effects of increased canalicular tortuosity on osteocyte stimulation

2.3.1. FSI model generation

Previous studies have investigated the role of proteoglycan PCM elements, which tether the osteocyte to the surrounding extracellular matrix (Han et al. 2004; You et al. 2004; You et al. 2001), and projections of the ECM into the canaliculi, which disturb the flow or attach directly to the cell process via integrin attachments (Anderson and Knothe Tate 2008; McNamara et al. 2009; Wang et al. 2007). To date no computational approach has been capable of modelling this complex multi-physics behaviour, incorporating both mechanisms into a full scale model of the osteocyte.

An FSI model of an idealised osteocyte lacuna was developed using ANSYS (Pittsburgh, Pennsylvania) multiphysics simulation software, similar to the methods described in detail previously (Verbruggen et al. 2013). The lacuna was modelled as an ellipsoid of minor and major axes 9 and 15 mm, respectively, while canaliculi were included as cylindrical channels of diameter 0.6 mm (Verbruggen et al. 2012). The osteocyte was also modelled as an ellipsoid with minor and major axes of 7.5 and 13.5 mm, respectively, surrounded by a PCM of thickness

0.75 mm (McNamara et al. 2009; You et al. 2004). The cell processes were created by offsetting from the canaliculi by 0.08 mm (Wang et al. 2005).

The ECM projections were modelled as conical protrusions, of height 0.08 µm and base radius 0.1 µm, which projected into the pericellular space in groups of four about the axis of the canaliculi (see Figure 2) (Wang et al. 2005). PCM tethering elements were included as cylinders of length 0.08 µm and radius 0.008 µm (Lemonnier et al. 2011; You et al. 2004), attaching the canalicular wall to the osteocyte cell process (Wang et al. 2005), and were organised in groups of eight about the axis of the canaliculi (see Figure 2). The ECM projections and PCM tethering elements were included at a spacing of 0.13 µm and 0.05 µm respectively, in order to closely represent their observed distribution in vivo (McNamara et al. 2009; You et al. 2004). Additionally, as the spacing of PCM tethering elements have been found to vary greatly, an analysis of the effect of PCM tether spacing was performed based on in vivo measurements using electron microscopy (0.012µm and 0.076 µm spacing) (You et al. 2004). Due to the small scale of PCM tethering elements and ECM projections, relative to the size of the osteocyte, it was necessary to employ symmetry boundary conditions to reduce computational cost. Thus, a model representing an octant of the osteocyte environment, as shown in Figure 2, was generated that could characterise strains in these features at a high resolution. These models were meshed with approximately 8.6 million ANSYS SOLID72 tetrahedral elements and exported to ANSYS.

2.3.2. Solid material and fluid properties

The material properties of the ECM and osteocyte were the same as those described in Section 2.2.1, with the ECM elastic modulus maintained at 16 GPa. The flexural rigidity (EI), defined as the product of the elastic modulus (E) and the moment of inertia (I), of PCM tethering elements has been determined previously as 700 $pNnm^2$ (Weinbaum et al. 2003). Assuming

that a PCM tethering element is a solid cylinder, its moment of inertia can be calculated as follows:

$$I = \frac{\pi r^4}{4}$$

where r is the radius of the PCM tethering element. Taking the experimentally determined radius of 8 nm for these fibres (Lemonnier et al. 2011; You et al. 2004), and dividing the flexural rigidity by the resulting moment of inertia, an elastic modulus of 2.18 MPa can be calculated for the PCM tethering elements. The Poisson's ratio was assumed to be 0.4, similar to the experimentally-derived properties of the actin cytoskeleton (Gittes et al. 1993). The properties of the interstitial fluid were assumed to be similar to water, with a density of 997 kgm^{-3} and a dynamic viscosity of 0.000855 $kgm^{-1}s^{-1}$ (Anderson et al. 2005). Flow within the lacunar-canalicular system was assumed to be laminar in nature.

2.3.3. Boundary conditions and loading

Similar boundary conditions were applied to those described previously (Verbruggen et al. 2013). Briefly, a compressive uni-axial load of 3,000 με was applied by means of a displacement boundary condition, while a pressure of 300 Pa was applied to the inlet on one face and the other openings are defined as outlets at a relative pressure of 0 Pa (Anderson et al. 2005; Knothe Tate and Niederer 1998; Manfredini et al. 1999). A staggered iteration FSI analysis was then conducted, as outlined in the authors' previous study (Verbruggen et al. 2013), with the results of this analysis interpolated onto the surface of the osteocyte to allow elucidation of the strain within the cell. Briefly, the deformations at the interface between the ECM and the pericellular fluid space resulting from the applied loading were mapped onto the fluid domain using a staggered iteration approach inherent in ANSYS coupling software. The resulting fluid equations were solved, and forces were relayed back to the solid ECM domain

as new boundary conditions, allowing gradual mesh motion and strongly coupled solution through further iterations. This method was performed repeatedly within each step until convergence of the field equations and a fully implicit solution was achieved. Upon solution of this FSI analysis, the loading-induced fluid flow was analysed. The pressure load on the surface of the cell membrane arising from the flow was then exported to ANSYS Structural and interpolated onto the surface of the solid osteocyte domain. This in turn allowed investigation of the deformation in the cell and PCM tethering elements resulting from the fluid flow imposed by global ECM loading.

2.3.4. Study of lacunar-canalicular tortuosity in osteoporosis

In order to investigate observed changes in the tortuosity of the lacunar-canalicular network during osteoporosis (Knothe Tate et al. 2002; Knothe Tate et al. 2004), an idealised osteocyte model was generated in which a more tortuous canalicular anatomy was included. As quantitative data on the degree of increased tortuosity in osteoporosis is not available, this was modelled by alternately adjusting the axis of one of the canaliculi by a 45° angle every 2 μm along its length, estimated from previously published research (Knothe Tate et al. 2002). In order to isolate the effect of this geometry from the amplifying effects of the PCM tethering elements and ECM projections, this tortuosity was applied in models both with and without these strain amplification mechanisms, which are described in detail above.

3. RESULTS

3.1. Are changes in osteocyte stimulation explained by altered bone tissue properties?

The temporal differences in the experimentally observed volume of the osteocyte cells stimulated above the osteogenic strain threshold (>10,000 με), between healthy (SHAM) and osteoporotic (OVX) bone, at both 5 and 34 weeks post-operation, are shown in Figure 3. The predictions of the computational models of this study are presented for the two extreme

scenarios (2 GPa and 4 GPa). This process is illustrated in Figure 4 using representative experimental images of SHAM and OVX osteocytes at 5 weeks of oestrogen post-operation (Verbruggen et al. 2015), comparing osteogenic strain stimulation to that in one of the four osteocyte FE models for which the elastic modulus was varied. This process was repeated until the mean of the experimental and computational strain stimulations matched, thus predicting the material properties of the bone matrix.

The predictions for the relevant ECM elastic moduli that most closely predict the experimental data for each of the experimental groups are provided and indicate that a decrease in elastic modulus from (2.75 GPa to 2.325 GPa) could explain the increase in strain stimulation quantified in the experimental groups (SHAM-5 to OVX-5). Conversely, an increase in predicted stiffness (2.325 GPa to 3.5 GPa) from early to late-stage oestrogen deficiency (comparing OVX-5 to OVX-34), such that it has a similar stiffness to the healthy bone (3.4 GPa) at the same time-point (SHAM-34), explains the increase in strain stimulation quantified in the experimental group (OVX-34).

3.2. Are changes in osteocyte stimulation explained by altered bone tissue mineralisation?

The mineral content, expressed as calcium content, calculated for the predicted tissue moduli are presented in Table 1 for control and oestrogen deficient groups at 5 and 34 weeks post-operation. These results indicate that, at 5 weeks post-OVX, a weight percentage decrease of 0.66 wt% Ca, corresponding to a decrease in elastic modulus of 0.425 GPa, compared to healthy bone at the same time-point, could explain the increased strain stimulation experienced by osteocytes during the early stages of osteoporosis. Similarly, by 34 weeks post-OVX the mineralisation was predicted to increase by 1.64%, to a value of 18.06 wt% Ca, representative

of a 1.175 GPa increase in stiffness, thus explaining the decreased strain stimulation at 34 weeks post-OVX observed experimentally (Verbruggen et al. 2015).

3.3. Are osteoporosis-related changes in osteocyte stimulation explained by altered canalicular tortuosity?

The velocity, shear stress and strain distributions experienced by osteocytes with a tortuous canalicular structure are compared to a non-tortuous anatomy in Figure 5. These results are graphed in Figures 6A, 6B and 7 for velocity, shear stress and strain respectively. This data demonstrates that a decrease in fluid velocity and shear stress stimulation occurs with a tortuous anatomy in the model without the PCM and ECM attachments. However, this effect appears negligible with the inclusion of the PCM and ECM attachments. An additional analysis, in which PCM tethering element spacing was varied between the observed maximum (0.076 µm) and minimum (0.012 µm), resulted in a 1.4% increase and a 2.2 % decrease in velocity compared to the mean spacing of 0.05 µm, respectively. Similarly, shear stress increased by 3.3% with maximum spacing and decreased by 3.1% with minimum spacing, compared to the mean spacing. In contrast, the strain stimulation experienced by the osteocyte can be seen to increase noticeably with a more tortuous geometry, both with and without the presence of PCM and ECM attachments. This strongly suggests that a more tortuous canalicular anatomy in osteoporosis increases the strain simulation of the osteocyte, and that this osteoporotic geometry effect is independent of PCM and ECM attachments. This change in osteogenic strain stimulation is compared in Figure 7 to the changes in osteogenic strains we observed experimentally. It can clearly be seen that, while a more tortuous anatomy in osteoporosis may contribute to increases in strain stimulation, it cannot completely account for the large increases observed experimentally.

4. DISCUSSION

This study employs finite element and fluid-structure interaction computational techniques to elucidate the mechanisms by which osteocytes are stimulated in vivo, in both healthy bone tissue and bone from an animal model of osteoporosis. By simulating mechanical loading, it was predicted that an initial decrease in tissue stiffness (0.425 GPa) and mineral content (0.66 wt% Ca) relative to controls could explain the mechanical stimulation observed at the early stages of oestrogen deficiency (5 weeks post-OVX) during in situ bone cell loading in an oestrogen-deficient rat model (Verbruggen et al. 2015). Moreover, it was found that a later increase in stiffness (1.175 GPa) and mineral content (1.64 wt% Ca) during long-term osteoporosis (34 weeks post-OVX), could explain the mechanical stimuli observed at a later time point due to the progression of osteoporosis (Verbruggen et al. 2015). Furthermore, canalicular tortuosity was shown to result in increased osteogenic (> 10,000 με) strain stimulation, although this increase was not large enough to explain observed experimental results of changes in the micromechanical environment of osteocytes in osteoporotic bone.

In order to replicate the intricate environment of the osteocyte, a number of assumptions were necessary. Based on studies of the nano-scale dimensions of canalicular channels, laminar uni-directional flow was assumed throughout the lacunar-canalicular network for the FSI models (Anderson et al. 2005; Cheng and Giordano 2002). Furthermore, all solid elements were assumed to be linear elastic isotropic materials for both the FE and FSI models, with properties derived assigned from experimentally-determined values (Deligianni and Apostolopoulos 2008; Sugawara et al. 2008; Weinbaum et al. 2003). In reality it would be expected that there would indeed be a non-linear relationship between loading and stimulation, due to the complex non-linear material properties of bone matrix and also the time-dependant interstitial fluid flow within the lacunar canalicular network. However, we have assumed linear elastic behaviour for the osteocyte due to its long relaxation time (41.5 s) relative to average

frequency of physiological loading (~1 s) (Appelman et al. 2011; Darling et al. 2008). It should also be noted that the elastic modulus variation study was investigated only using a finite element approach as it is not known how changes in tissue composition could alter the boundary conditions on the fluid flow within the PCM. Incorporation of this effect on fluid flow could potentially alter the stimulation effects of changes in tissue properties in a full FSI simulation. However, further experimental studies are required to firmly establish the link between bone tissue properties and loading-induced fluid flow. While the spacing of PCM tethering elements has been found to vary greatly (You et al. 2004), our results indicate that the spacing of the tethering elements within the in vivo range (12 nm and 76 nm spacing) does not have a large effect on stimulation. Additionally, a recent study of these tethering elements using AFM has determined the diameter to be narrower than previously thought, at 2-4 nm, which could affect the behaviour of the elements predicted in the current study (Wijeratne et al. 2016; You et al. 2004). However, modelling each tethering element at 4 nm diameter with sufficient mesh density would require further millions of elements, and as such would be prohibitively computationally challenging. Furthermore, while increased tortuosity (Knothe Tate et al. 2002; Knothe Tate et al. 2004) has been indicated by experimental observations using 3D reconstructed histological sections, such changes have not been quantified sufficiently due to limitations caused by current imaging and sectioning techniques. As such, the presence of tortuosity were estimated in the models shown here, and further experimental studies using techniques such as TEM imaging to quantitatively determine these changes (McNamara et al. 2009), as well as alterations in the PCM and number of canaliculi, are required to inform future models that can investigate these questions further. Indeed, recent advances in imaging technologies, such as acid etching techniques (Milovanovic et al. 2013) and X-ray nano-tomography (Varga et al. 2015) have allowed for the highly detailed

investigations of lacunar-canalicular geometry, which could be applied to investigate the environment of osteocytes during osteoporosis in future studies.

Our previous experimental study showed that osteocytes in osteoporotic bone initially (5 weeks) experience osteogenic strains (>10,000 με) in a greater area of the cell than those in healthy bone (Verbruggen et al. 2015). In contrast, in long-term oestrogen deficiency (i.e. by 34 weeks after OVX) there was a significant decrease in the proportion of osteoporotic osteocytes exceeding this threshold, such that there was no longer a significant difference between osteocytes in 34-week osteoporotic and healthy bone (Verbruggen et al. 2015). We proposed that a cell-driven mechanobiological response may occur due to the increased stimulation experienced in early oestrogen deficiency, and that this response may manifest as increased bone tissue stiffness and mineralisation, a phenomenon that has been observed in trabecular bone from animal models of osteoporosis (Brennan et al. 2011a; McNamara et al. 2006). In the current study, finite element models with representative osteocyte geometries were employed to determine whether our observed changes in osteocyte mechanical stimulation could indeed be explained by alterations in bone tissue stiffness and mineralisation during oestrogen deficiency. By varying the elastic modulus of the ECM in the models to achieve strains within the ranges observed in the experimental study for each group, it was predicted that an initial decrease in tissue stiffness of 0.425 GPa relative to controls could explain the mechanical stimuli observed experimentally at the early stages of oestrogen deficiency (5 weeks post-OVX). Moreover, it was found that a later increase in stiffness of 1.175 GPa during long-term osteoporosis, could explain the mechanical stimuli observed experimentally at the later time point (34 weeks post-OVX). Interestingly, previous experimental studies have reported temporal changes in bone tissue stiffness of trabeculae from a rat model of osteoporosis (McNamara et al. 2006). By 14 weeks post-operation, the stiffness of OVX tissue was found to increase significantly compared to controls (5.11 vs. 2.67 GPa),

with this stiffness later decreasing to match controls by 54 weeks post-OVX (McNamara et al. 2006). Furthermore, it has been reported in an ovine model of osteoporosis that initial (12 months post-OVX) decreases in mineral content and stiffness (by 2.1 wt% Ca and 3.4 GPa, respectively) before increasing (by 0.6 wt% Ca and 0.7 GPa, respectively) to match control values in late-stage osteoporosis (31 months post-OVX) (Brennan et al. 2009; Brennan et al. 2011b). Similarly, cortical bone in ovine studies has been observed to result in decreased stiffness (by 1.7 GPa) in early (12 months post-OVX) osteoporosis (Kennedy et al. 2009). These ovine studies also found that, as the animals progressed into long-term oestrogen deficiency, there was no significant difference in cortical compressive strength by 31 months post-OVX (Healy et al. 2010; Kennedy et al. 2009).

Although the qualitative changes in tissue properties in trabecular and cortical bone from previous experimental studies would appear to corroborate the predictions of the models in the current study, the magnitude of changes are not the same, which might be explained by differences in the animal models (rat vs. sheep) or time points. Nonetheless, these experimental results appear to confirm our hypothesis that a compensatory mechanobiological response occurs in response to initial increased loading (due to bone loss), whereby an increase in tissue mineral content and stiffness occur to reduce this loading. However, following ovariectomy there is a significant depletion of bone architecture and, as mineral can only be laid down in the remaining trabeculae and trabeculae cannot be reconnected, the bone mass is not restored (Keiler et al. 2012). Furthermore, it has been proposed that these changes in stiffness during osteoporosis could be the result of increased mineralisation (McNamara 2010). Conversion of the elastic moduli in the current study to mineral content demonstrates a corresponding initial significant decrease in mineralisation of 0.66 wt% Ca, followed by later increase of 1.64 wt% Ca, such that there is no significant difference compared to controls (17.94 vs. 18.06 wt% Ca). This same trend, with an initial decrease (2.1 wt% Ca) followed by a subsequent increase (0.6

wt% Ca), was observed in an ovine model of temporal changes in mineralisation during osteoporosis (Brennan et al. 2009; Brennan et al. 2011b). Future studies could use similar techniques to further investigate the connection between mineralisation and in vivo osteocyte stimulation. The predictions of the models in the current study demonstrate that observed osteoporotic changes in tissue properties and mineralisation may be correlated to osteocyte stimulation, elucidating a possible mechanobiological link between the cellular environment and macroscopic bone properties in the development of osteoporosis.

One significant alteration to the osteocyte environment, which has been shown to occur in osteoporosis, is an increase in tortuosity of the canaliculi (Knothe Tate et al. 2002; Knothe Tate et al. 2004). By applying computational modelling approaches we predicted that such changes can lead to an increase in osteogenic strain stimulation of osteocytes, both with and without cellular attachments. These results reinforce our previous findings that osteocytes are highly sensitive to changes in canalicular geometry (Verbruggen et al. 2012), and suggest that canalicular tortuosity may be a mechanism by which osteocytes may sense osteoporotic changes. However, when compared to the increases in osteogenic strain stimulation observed in our experimental study it was seen that, while tortuosity may contribute, it cannot completely explain the difference in osteoporosis. Moreover, it is not known whether this increased tortuosity is a direct response to oestrogen deficiency, or whether the canalicular geometry is altered by the osteocytes themselves when the loading environment is altered during osteoporosis, in order to heighten sensitivity to strain (Harris et al. 2007). Similarly, these changes could arise due to alteration in the mineralisation of the lamina limitans (Takagi et al. 1991). The observed increases in tortuosity may also be caused by a "slackening" or structural change in the cell processes themselves, with resulting alterations to the canalicular geometry, although this has not been directly observed. As the order in which these changes arise during the progression of osteoporosis is not understood, further studies which illuminate the temporal

changes in canalicular anatomy during disease may provide a greater understanding of the development of this feature.

5. CONCLUSION

The results of this study determined the effect of bone tissue stiffness and mineralisation on osteocyte stimulation, thus elucidating a possible mechanobiological link in the temporal development of osteoporosis. Furthermore, osteoporosis-related canalicular tortuosity was shown to result in increased osteogenic strain stimulation, though to a lesser extent than that observed experimentally. This research indicated that the changes in the extracellular environment during osteoporosis, arising from altered mineralisation and lacunar-canalicular architecture, lead to altered mechanical stimulation of osteoblasts and osteocytes. The findings of this study provide a novel insight into the complex in vivo mechanical environment of osteocytes and elucidate how specific changes in the extracellular environment alter the mechanical stimulation of osteocytes during osteoporosis. Moreover, the findings complement our previously developed experimental approach, and together provide a novel insight into the osteocyte environment in both healthy bone and during the disease of osteoporosis.

6. ACKNOWLEDGEMENTS

The authors would like to acknowledge funding from the Irish Research Council (IRC) under the EMBARK program (S. W. V.), the European Research Council (ERC) under grant number 258992 (BONEMECHBIO) and the Irish Centre for High-End Computing (ICHEC).

7. REFERENCES

Ajubi NE, Klein-Nulend J, Nijweide PJ, Vrijheid-Lammers T, Alblas MJ, Burger EH (1996) Pulsating Fluid Flow Increases Prostaglandin Production by Cultured Chicken Osteocytes—A Cytoskeleton-Dependent Process Biochemical and Biophysical Research Communications 225:62-68 doi:10.1006/bbrc.1996.1131

Alexopoulos LG, Haider MA, Vail TP, Guilak F (2003) Alterations in the Mechanical Properties of the Human Chondrocyte Pericellular Matrix With Osteoarthritis Journal of Biomechanical Engineering 125:323-333

Alexopoulos LG, Setton LA, Guilak F (2005) The biomechanical role of the chondrocyte pericellular matrix in articular cartilage Acta Biomaterialia 1:317-325

Anderson E, Kaliyamoorthy S, Alexander J, Tate M (2005) Nano–Microscale Models of Periosteocytic Flow Show Differences in Stresses Imparted to Cell Body and Processes Annals of Biomedical Engineering 33:52-62 doi:10.1007/s10439-005-8962-y

Anderson EJ, Knothe Tate ML (2008) Idealization of pericellular fluid space geometry and dimension results in a profound underprediction of nano-microscale stresses imparted by fluid drag on osteocytes Journal of Biomechanics 41:1736-1746

Appelman TP, Mizrahi J, Seliktar D (2011) A Finite Element Model of Cell-Matrix Interactions to Study the Differential Effect of Scaffold Composition on Chondrogenic Response to Mechanical Stimulation Journal of Biomechanical Engineering 133:041010-041012

Brennan MA, Gleeson JP, Browne M, O'Brien FJ, Thurner PJ, McNamara LM (2011a) Site specific increase in heterogeneity of trabecular bone tissue mineral during oestrogen deficiency Eur Cell Mater 21:396-406 doi:vol021a30 [pii]

Brennan O, Kennedy OD, Lee TC, Rackard SM, O'Brien FJ (2009) Biomechanical properties across trabeculae from the proximal femur of normal and ovariectomised sheep Journal of Biomechanics 42:498-503 doi:http://dx.doi.org/10.1016/j.jbiomech.2008.11.032

Brennan O, Kennedy OD, Lee TC, Rackard SM, O'Brien FJ, McNamara LM (2011b) The effects of estrogen deficiency and bisphosphonate treatment on tissue mineralisation and stiffness in an ovine model of osteoporosis Journal of Biomechanics 44:386-390 doi:http://dx.doi.org/10.1016/j.jbiomech.2010.10.023

Brennan O, Kuliwaba J, Lee TC, Parkinson I, Fazzalari N, McNamara L, O'Brien F (2012) Temporal Changes in Bone Composition, Architecture, and Strength Following Estrogen Deficiency in Osteoporosis Calcif Tissue Int 91:440-449 doi:10.1007/s00223-012-9657-7

Burger EH, Veldhuijzen JP (1993a) Influence of mechanical factors on bone formation, resorption and growth in vitro Bone 7:37-56

Burger EH, Veldhuijzen JP (1993b) Influence of mechanical factors on bone formation, resorption and growth in vitro vol 7. Bone. CRC Press Boca Raton, FL.,

Busse B, Hahn M, Soltau M, Zustin J, Püschel K, Duda GN, Amling M (2009) Increased calcium content and inhomogeneity of mineralization render bone toughness in osteoporosis: Mineralization, morphology and biomechanics of human single trabeculae Bone 45:1034-1043 doi:http://dx.doi.org/10.1016/j.bone.2009.08.002

Carter DR, Caler WE (1985) A cumulative damage model for bone fracture Journal of Orthopaedic Research 3:84-90 doi:10.1002/jor.1100030110

Cheng JT, Giordano N (2002) Fluid flow through nanometer-scale channels Physical Review E 65:031206

Compston JE, Mellish RWE, Croucher P, Newcombe R, Garrahan NJ (1989) Structural mechanisms of trabecular bone loss in man Bone and Mineral 6:339-350 doi:10.1016/0169-6009(89)90039-1

Cowin SC, Moss-Salentijn L, Moss ML (1991) Candidates for the mechanosensory system in bone Journal of Biomechanical Engineering 113:191

Currey JD (1988) The effect of porosity and mineral content on the Young's modulus of elasticity of compact bone Journal of Biomechanics 21:131-139

Darling EM, Topel M, Zauscher S, Vail TP, Guilak F (2008) Viscoelastic properties of human mesenchymally-derived stem cells and primary osteoblasts, chondrocytes, and adipocytes Journal of Biomechanics 41:454-464

Deligianni D, Apostolopoulos C (2008) Multilevel finite element modeling for the prediction of local cellular deformation in bone Biomech Model Mechanobiol 7:151-159 doi:10.1007/s10237-007-0082-1

Fritton SP, J. McLeod K, Rubin CT (2000) Quantifying the strain history of bone: spatial uniformity and self-similarity of low-magnitude strains Journal of Biomechanics 33:317-325

Gittes F, Mickey B, Nettleton J, Howard J (1993) Flexural rigidity of microtubules and actin filaments measured from thermal fluctuations in shape The Journal of Cell Biology 120:923-934 doi:10.1083/jcb.120.4.923

Han Y, Cowin SC, Schaffler MB, Weinbaum S (2004) Mechanotransduction and strain amplification in osteocyte cell processes Proceedings of the National Academy of Sciences of the United States of America 101:16689-16694 doi:10.1073/pnas.0407429101

Harris S et al. (2007) DMP1 and MEPE expression are elevated in osteocytes after mechanical loading in vivo: theoretical role in controlling mineral quality in the perilacunar matrix Journal of musculoskeletal & neuronal interactions 7:313

Healy C, Kennedy OD, Brennan O, Rackard SM, O'Brien FJ, Lee TC (2010) Structural adaptation and intracortical bone turnover in an ovine model of osteoporosis Journal of Orthopaedic Research 28:248-251 doi:10.1002/jor.20961

Huiskes R, Ruimerman R, Van Lenthe GH, Janssen JD (2000) Effects of mechanical forces on maintenance and adaptation of form in trabecular bone Nature 405:704-706

Kamioka H et al. (2012) Microscale fluid flow analysis in a human osteocyte canaliculus using a realistic high-resolution image-based three-dimensional model Integrative Biology

Keiler AM, Zierau O, Vollmer G, Scharnweber D, Bernhardt R (2012) Estimation of an early meaningful time point of bone parameter changes in application to an osteoporotic rat model with in vivo microcomputed tomography measurements Laboratory Animals 46:237-244

Kennedy OD, Brennan O, Rackard SM, Staines A, O'Brien FJ, Taylor D, Lee TC (2009) Effects of ovariectomy on bone turnover, porosity, and biomechanical properties in ovine compact bone 12 months postsurgery Journal of Orthopaedic Research 27:303-309 doi:10.1002/jor.20750

Klein-Nulend J, van der Plas A, Semeins CM, Ajubi NE, Frangos JA, Nijweide PJ, Burger EH (1995) Sensitivity of osteocytes to biomechanical stress in vitro The FASEB Journal 9:441-445

Knothe Tate M, Tami A, Bauer T, Knothe U (2002) Micropathoanatomy of osteoporosis: indications for a cellular basis of bone disease Advances in Osteoporotic Fracture Management 2:9-14

Knothe Tate ML, Adamson JR, Tami AE, Bauer TW (2004) The osteocyte The international journal of biochemistry & cell biology 36:1-8

Knothe Tate ML, Niederer P (1998) A theoretical FE-base model developed to predict the relative contribution of convective and diffusive transport mechanisms for the maintenance of local equilibria within cortical bone. Paper presented at the Advances in Heat and Mass Transfer in Biotechnology, Anaheim, California,

Lanyon LE (1993) Osteocytes, strain detection, bone modeling and remodeling Calcif Tissue Int 53:S102-S107 doi:10.1007/bf01673415

Lemonnier S, Naili S, Oddou C, Lemaire T (2011) Numerical determination of the lacuno-canalicular permeability of bone Computer Methods in Biomechanics and Biomedical Engineering 14:133-135 doi:10.1080/10255842.2011.593767

Manfredini P, Cocchetti G, Maier G, Redaelli A, Montevecchi FM (1999) Poroelastic finite element analysis of a bone specimen under cyclic loading Journal of Biomechanics 32:135-144

McNamara LM (2010) Perspective on post-menopausal osteoporosis: establishing an interdisciplinary understanding of the sequence of events from the molecular level to whole bone fractures Journal of The Royal Society Interface 7:353-372 doi:10.1098/rsif.2009.0282

McNamara LM, Ederveen AGH, Lyons CG, Price C, Schaffler MB, Weinans H, Prendergast PJ (2006) Strength of cancellous bone trabecular tissue from normal, ovariectomized and drug-treated rats over the course of ageing Bone 39:392-400 doi:10.1016/j.bone.2006.02.070

McNamara LM, Majeska RJ, Weinbaum S, Friedrich V, Schaffler MB (2009) Attachment of Osteocyte Cell Processes to the Bone Matrix The Anatomical Record: Advances in Integrative Anatomy and Evolutionary Biology 292:355-363 doi:10.1002/ar.20869

McNamara LM, Prendergast PJ (2005) Perforation of cancellous bone trabeculae by damage-stimulated remodelling at resorption pits: a computational analysis Eur J Morphol 42:99-109 doi:J7N4U41T77053P67 [pii]

10.1080/09243860500096289

Milovanovic P et al. (2013) Osteocytic Canalicular Networks: Morphological Implications for Altered Mechanosensitivity ACS Nano 7:7542-7551 doi:10.1021/nn401360u

Mullender M, Huiskes R (1995) Proposal for the regulatory mechanism of Wolff's law Journal of orthopaedic research 13:503-512

Mullender M, Huiskes R (1997) Osteocytes and bone lining cells: which are the best candidates for mechano-sensors in cancellous bone? Bone 20:527-532

Mullender M, Huiskes R, Weinans H (1994) A physiological approach to the simulation of bone remodeling as a self-organizational control process Journal of Biomechanics 27:1389-1394

Parfitt AM (1987) Bone Remodeling and Bone Loss: Understanding The Pathophysiology of Osteoporosis Clinical Obstetrics and Gynecology 30:789-811

Sauren YM, Mieremet RH, Groot CG, Scherft JP (1992) An electron microscopic study on the presence of proteoglycans in the mineralized matrix of rat and human compact lamellar bone The Anatomical Record 232:36-44

Smit TH, Burger EH (2000) Is BMU-Coupling a Strain-Regulated Phenomenon? A Finite Element Analysis Journal of Bone and Mineral Research 15:301-307 doi:10.1359/jbmr.2000.15.2.301

Sugawara Y et al. (2008) The alteration of a mechanical property of bone cells during the process of changing from osteoblasts to osteocytes Bone 43:19-24

Takagi M, Maeno M, Kagami A, Takahashi Y, Otsuka K (1991) Biochemical and immunocytochemical characterization of mineral binding proteoglycans in rat bone Journal of Histochemistry & Cytochemistry 39:41-50 doi:10.1177/39.1.1898498

Varga P et al. (2015) Synchrotron X-ray phase nano-tomography-based analysis of the lacunar–canalicular network morphology and its relation to the strains experienced by osteocytes in situ as predicted by case-specific finite element analysis Biomech Model Mechanobiol 14:267-282 doi:10.1007/s10237-014-0601-9

Verbruggen Stefaan W, Mc Garrigle Myles J, Haugh Matthew G, Voisin Muriel C, McNamara Laoise M (2015) Altered Mechanical Environment of Bone Cells in an Animal Model

of Short- and Long-Term Osteoporosis Biophysical Journal 108:1587-1598 doi:http://dx.doi.org/10.1016/j.bpj.2015.02.031

Verbruggen SW, Vaughan TJ, McNamara LM (2012) Strain amplification in bone mechanobiology: a computational investigation of the in vivo mechanics of osteocytes Journal of The Royal Society Interface doi:10.1098/rsif.2012.0286

Verbruggen SW, Vaughan TJ, McNamara LM (2013) Fluid flow in the osteocyte mechanical environment: a fluid–structure interaction approach Biomech Model Mechanobiol:1-13 doi:10.1007/s10237-013-0487-y

Wang L, Wang Y, Han Y, Henderson SC, Majeska RJ, Weinbaum S, Schaffler MB (2005) In situ measurement of solute transport in the bone lacunar-canalicular system Proceedings of the National Academy of Sciences of the United States of America 102:11911-11916 doi:10.1073/pnas.0505193102

Wang Y, McNamara LM, Schaffler MB, Weinbaum S (2007) A model for the role of integrins in flow induced mechanotransduction in osteocytes Proceedings of the National Academy of Sciences 104:15941-15946 doi:10.1073/pnas.0707246104

Weinbaum S, Cowin SC, Zeng Y (1994) A model for the excitation of osteocytes by mechanical loading-induced bone fluid shear stresses Journal of Biomechanics 27:339-360

Weinbaum S, Zhang X, Han Y, Vink H, Cowin SC (2003) Mechanotransduction and flow across the endothelial glycocalyx Proceedings of the National Academy of Sciences 100:7988-7995 doi:10.1073/pnas.1332808100

Westbroek I, Ajubi NE, Alblas MJ, Semeins CM, Klein-Nulend J, Burger EH, Nijweide PJ (2000) Differential Stimulation of Prostaglandin G/H Synthase-2 in Osteocytes and Other Osteogenic Cells by Pulsating Fluid Flow Biochemical and Biophysical Research Communications 268:414-419 doi:10.1006/bbrc.2000.2154

Wijeratne SS et al. (2016) Single molecule force measurements of perlecan/HSPG2: A key component of the osteocyte pericellular matrix Matrix Biology 50:27-38 doi:http://dx.doi.org/10.1016/j.matbio.2015.11.001

Wilusz RE, Sanchez-Adams J, Guilak F (2014) The structure and function of the pericellular matrix of articular cartilage Matrix Biology 39:25-32 doi:http://dx.doi.org/10.1016/j.matbio.2014.08.009

You J, Yellowley CE, Donahue HJ, Zhang Y, Chen Q, Jacobs CR (2000) Substrate Deformation Levels Associated With Routine Physical Activity Are Less Stimulatory to Bone Cells Relative to Loading-Induced Oscillatory Fluid Flow Journal of Biomechanical Engineering 122:387-393

You L-D, Weinbaum S, Cowin SC, Schaffler MB (2004) Ultrastructure of the osteocyte process and its pericellular matrix The Anatomical Record Part A: Discoveries in Molecular, Cellular, and Evolutionary Biology 278A:505-513 doi:10.1002/ar.a.20050

You L, Cowin SC, Schaffler MB, Weinbaum S (2001) A model for strain amplification in the actin cytoskeleton of osteocytes due to fluid drag on pericellular matrix Journal of Biomechanics 34:1375-1386

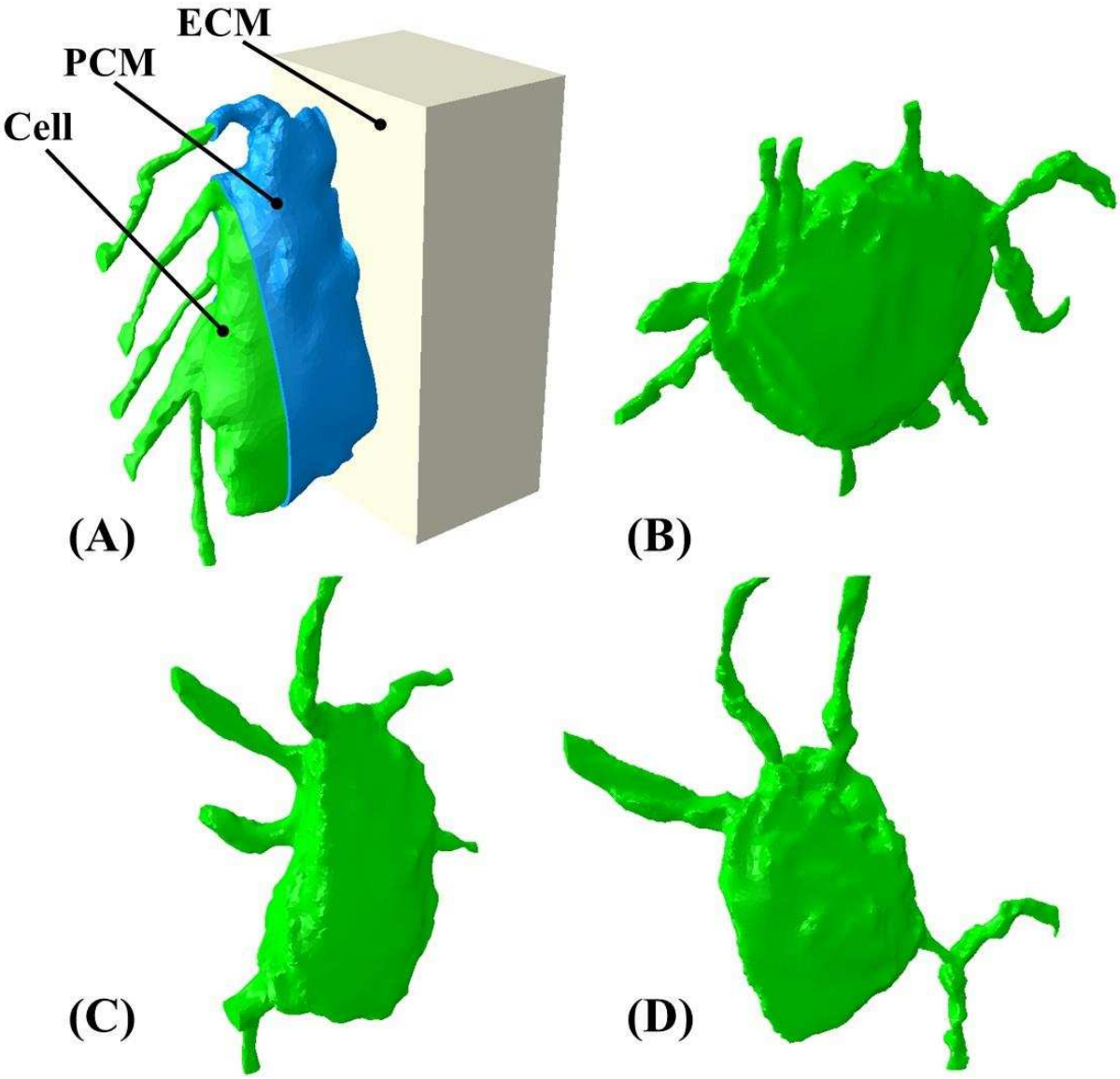

Figure 1: Diagram of confocal image-derived osteocyte models used in the finite element (FE) simulations (A-D) showing with the grey ECM, blue PCM and green cell visible shown (A).

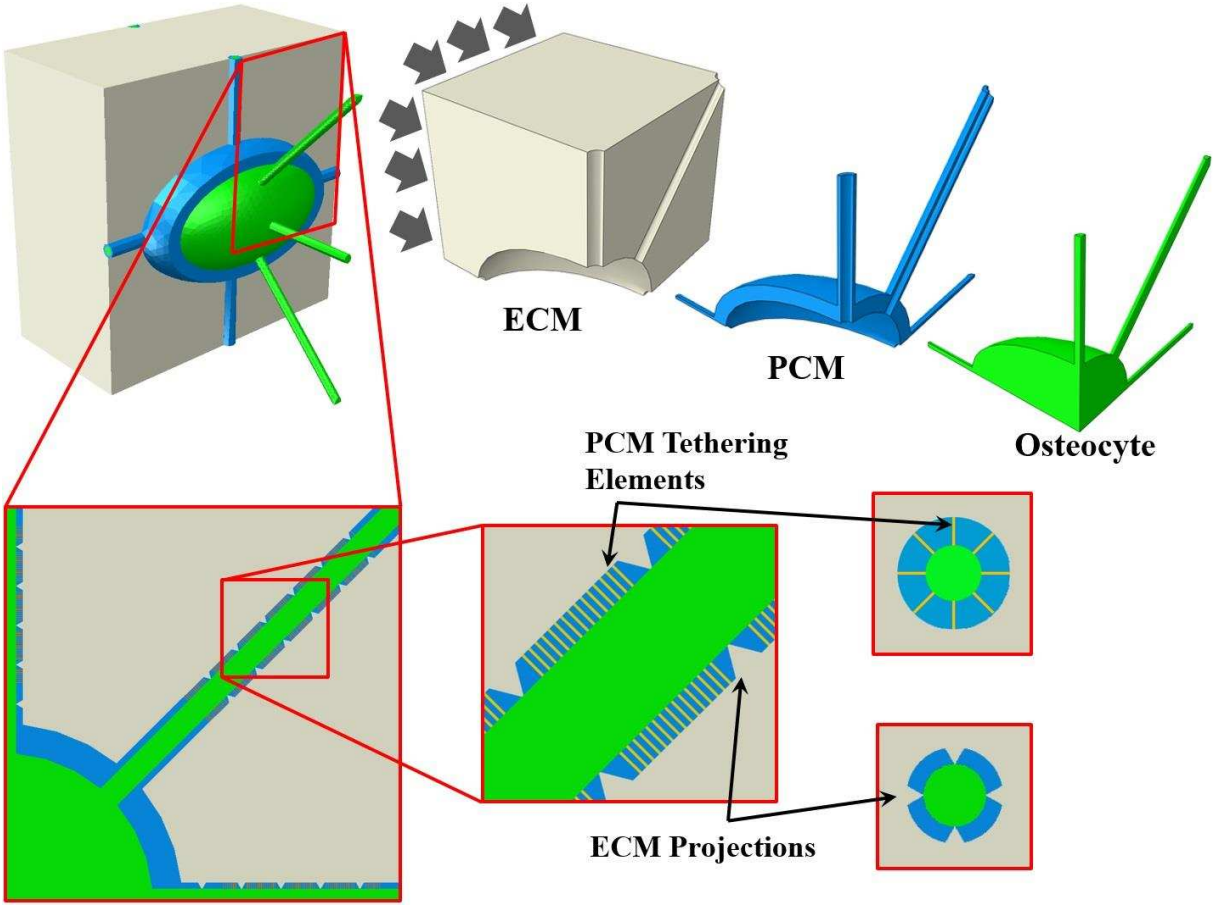

Figure 2: Diagram of osteocyte model used in the fluid-structure interaction (FSI) simulations, showing the three components of the osteocyte environment (ECM, PCM, Osteocyte) modelled as an octant using symmetry. Arrows indicate loading direction and the face on which it is applied. The location and arrangement of the PCM tethering elements and ECM projections is also indicated.

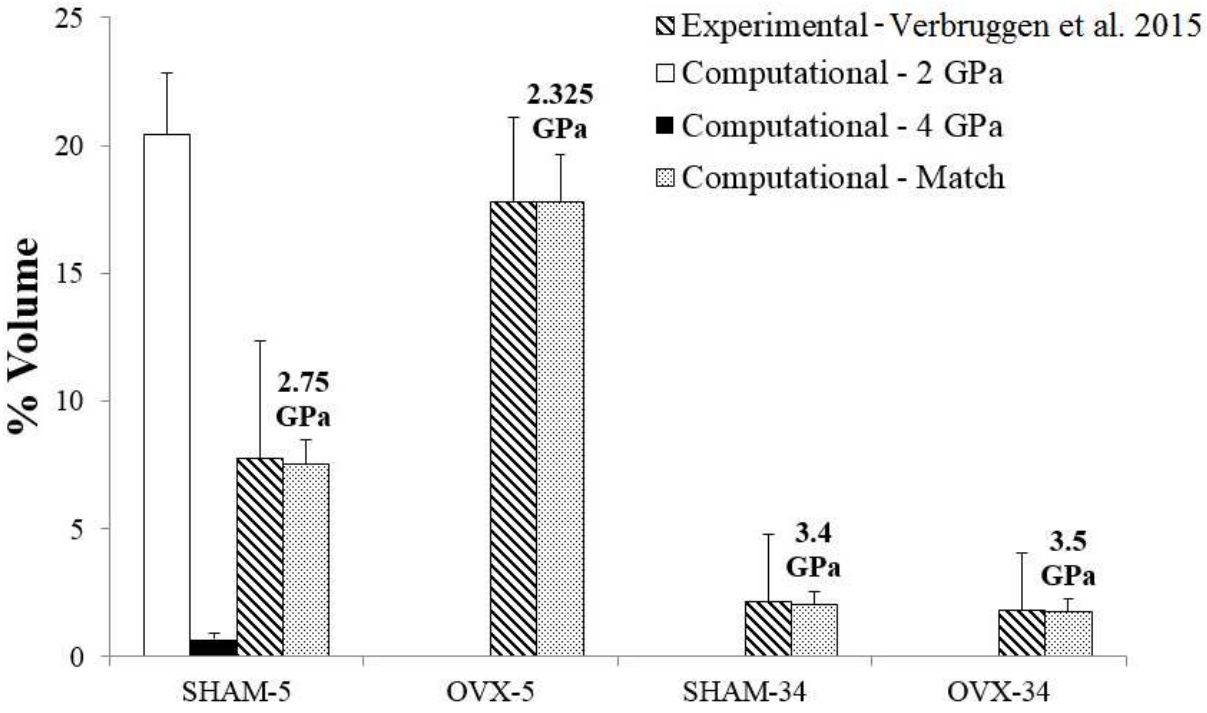

Figure 3: Strain distribution in computational models at various degrees of stiffness (highlighted above their respective data), alongside the strain distributions observed previously (Verbruggen et al. 2015), at various stages of both health and oestrogen deficiency. Osteogenic strain stimulation is shown for the maximum and minimum values (2 and 4 GPa) of the range within which the modulus was varied.

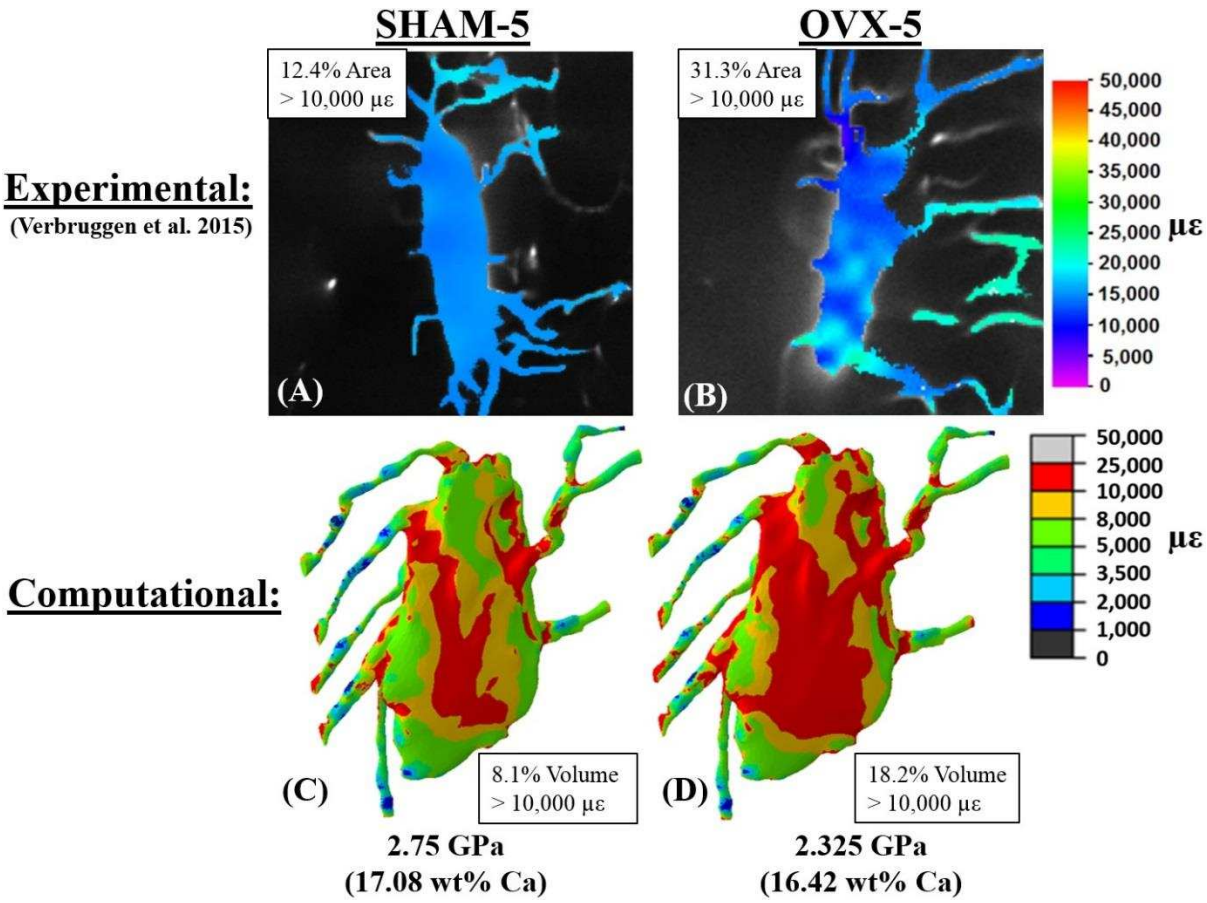

Figure 4: Representative images illustrating (A, B) an increase in strain stimulation between individual SHAM and OVX osteocytes at five weeks post-operation (Verbruggen et al. 2015), and (C, D) a similar increase in strain stimulation in one of the four FE models. The elastic moduli of the four computational models were varied until the mean strain stimulation matched that of the experimental data, resulting in the elastic moduli and mineral content predicted here.

	Elastic Modulus E (GPa)	Calcium Ca (mg/g)	Weight Percentage (wt% Ca)
SHAM-5	2.75	170.76	17.08
OVX-5	2.325	164.23	16.42
SHAM-34	3.4	179.40	17.94
OVX-34	3.5	180.62	18.06

Table 1: Differences in elastic modulus and calcium content based on experimentally observed cell strains.

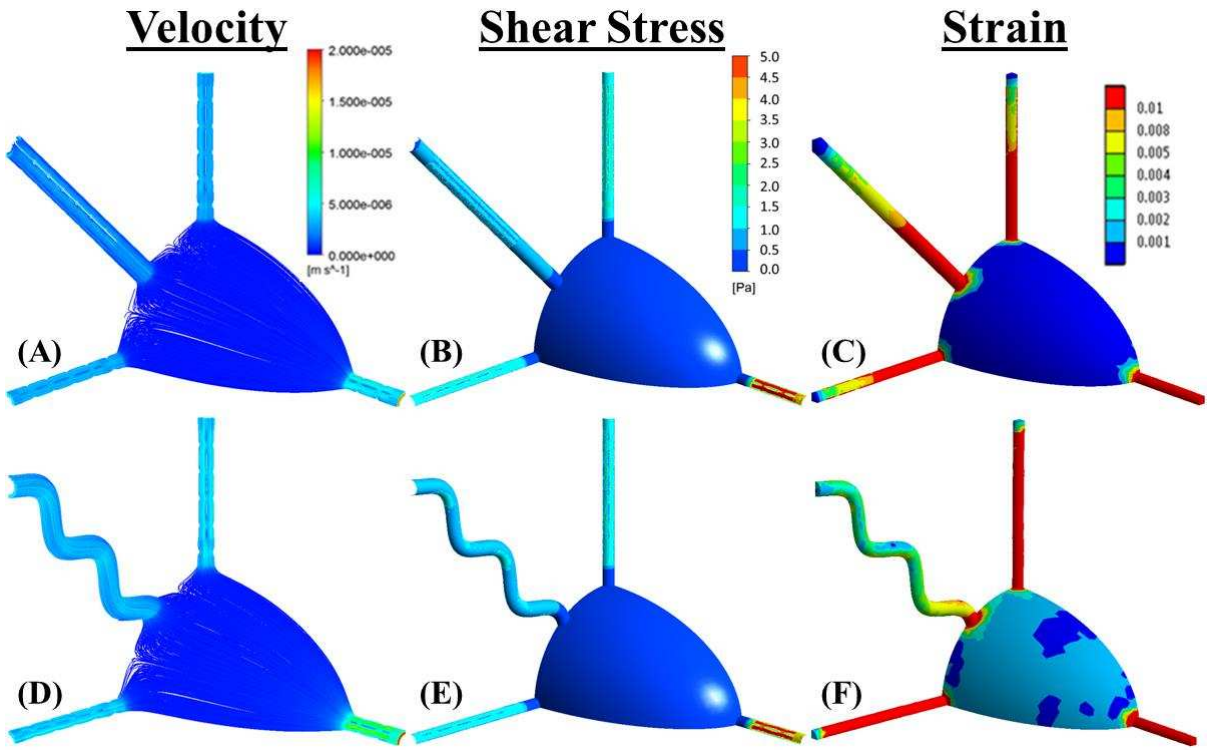

Figure 5: Changes in velocity, shear stress and strain distribution in models with cellular attachments (A-C), and also with a more tortuous anatomy, representative of osteoporosis (Knothe Tate et al. 2002; Knothe Tate et al. 2004) (D-F)

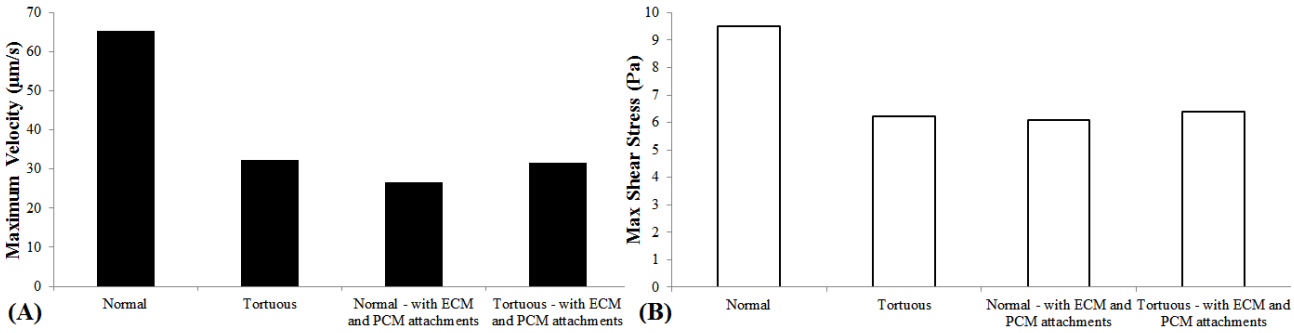

Figure 6: Effects of a more tortuous canalicular anatomy on (A) velocity and (B) shear stress, both with and without ECM and PCM attachments

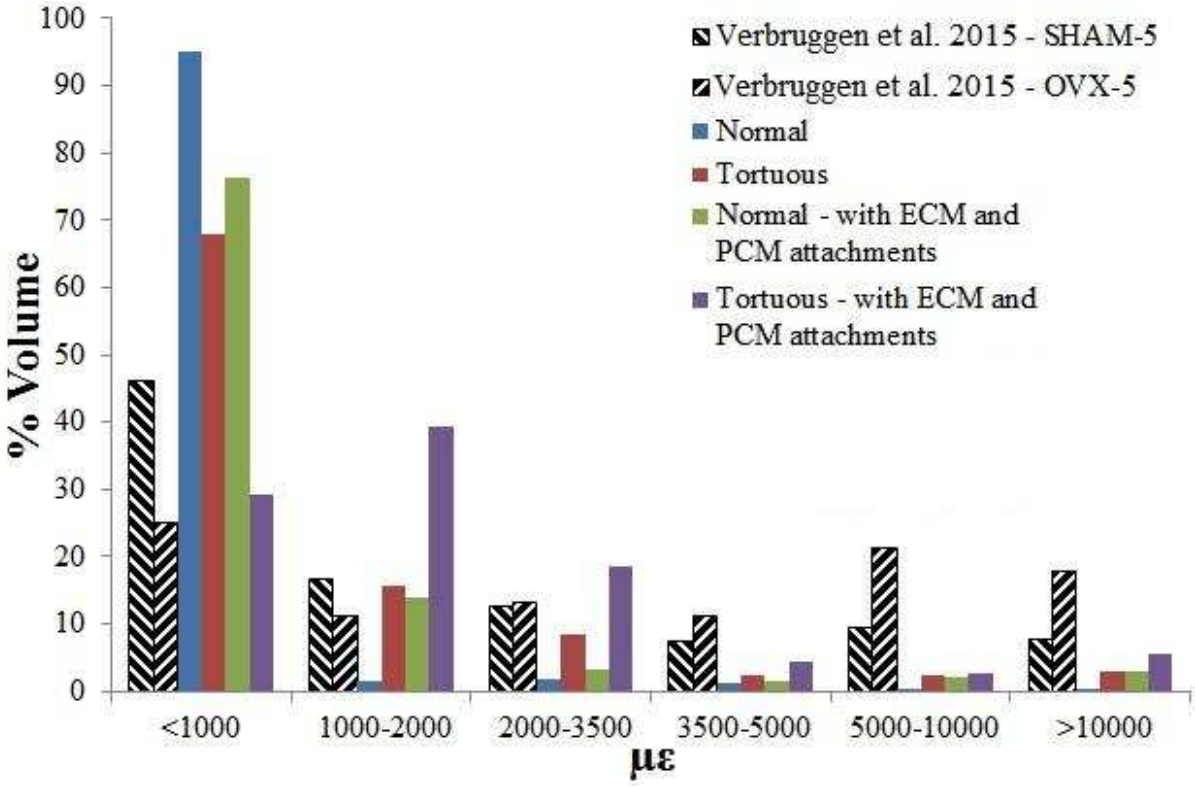

Figure 7: Effects of a more tortuous canalicular anatomy on strain distribution within an idealised osteocyte model, both with and without ECM and PCM attachments. Strain stimulation observed experimentally is also shown for context, for healthy and oestrogen deficient bone (Verbruggen et al. 2015).